International Conference on Hydraulics, Pneumatics, Sealing Elements, Precision Mechanics, Tools, Specific Electronic Equipment & Mechatronics
HERVEX 2023

Baile Govora, ROMANIA | 8-10 November, 2023

A milestone moment:
CELEBRATING
30 YEARS TOGETHER!

IMPACT VELOCITY CONTROL OF HOPKINSON BAR MECHATRONICS SYSTEM USING DRIVING ROBUST PRESSURE, NUMERICAL CALIBRATION, STRAIN WAVE MEASUREMENT AND INVERSE ANALYSIS

Author(s): Adinel GAVRUS

Affiliation: INSA Rennes (France)


PARIS
RENNES


INSA ROUEN
INSA STRASBOURG
INSA CENTRE VAL DE LOIRE
INSA LYON
INSA TOULOUSE
INSA Euro-Méditerranée
Fès | Maroc
UEMF

Contents

1. Introduction

Industrial Processes under Severe or Complex Loadings: Rapid Forging, High Speed Machining, Friction or Laser Welding, Automative Crash, Impact, …

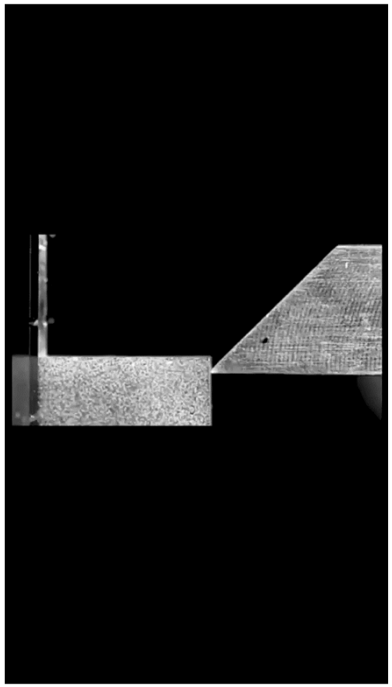

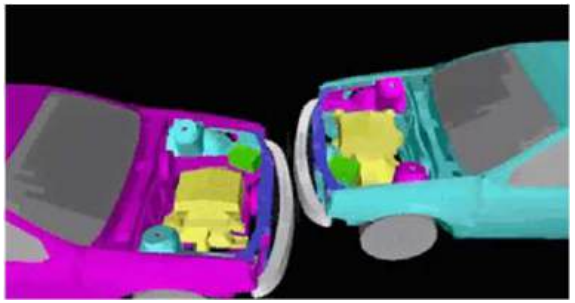

Process Optimisation using Numerical Simulation

$\bar{\sigma} = \sigma_0\left(\bar{\varepsilon}, \dot{\bar{\varepsilon}}, T, \ldots\right)$ **for** $\dot{\bar{\varepsilon}} \propto \boldsymbol{v}_{car} / \boldsymbol{l}_{car} \in \left[10^{-3}\boldsymbol{s}^{-1}, 10^{5}\boldsymbol{s}^{-1}\right]$

2. Pneumatic SHPB Mechatronics System

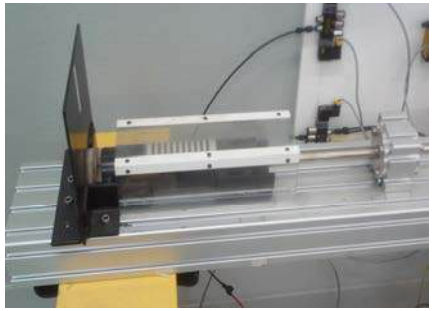

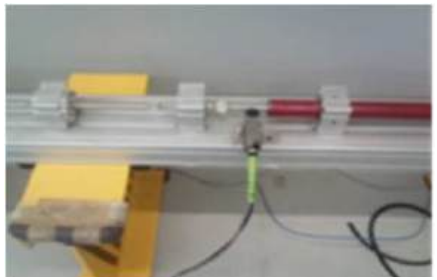

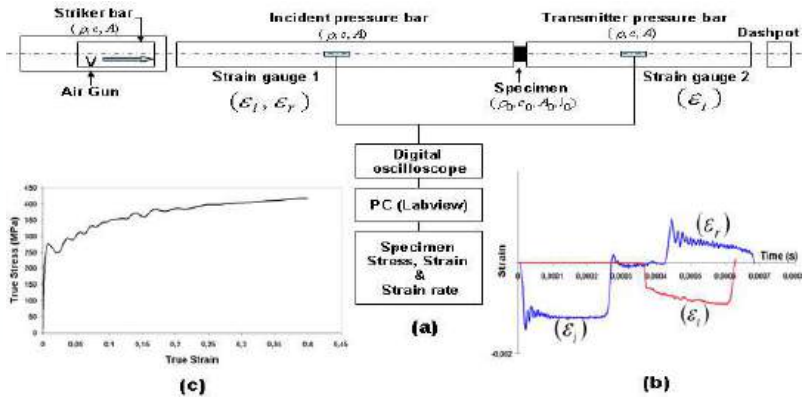

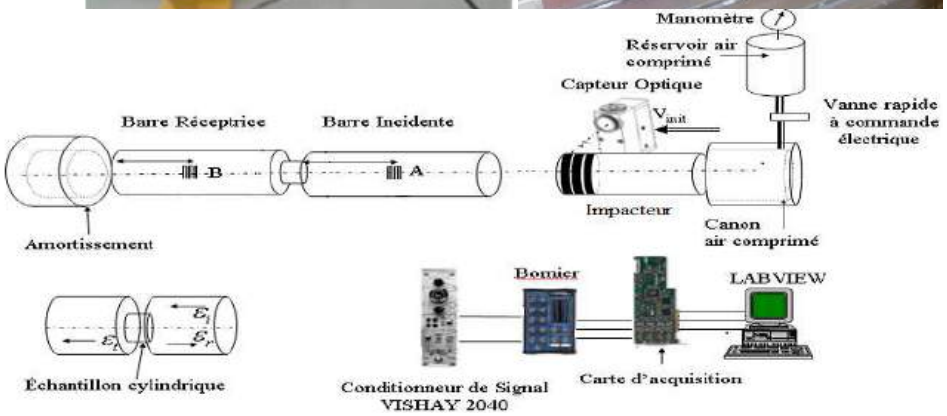

2.1 Framework and SHPB design characteristics

Table 1: Material and geometric characteristics of SHPB bars (total length of bench support ≈ 5,5 m)

Bars	Air Gun	Striker Bar	Receiving Bar	Sending Bar
Material	MARVAL 18	MARVAL 18	MARVAL 18	MARVAL 18
Diameter [mm]	ϕ_{in} 30.0 and ϕ_{out} 40.0	ϕ 16.0	ϕ 16.0	ϕ 16.0
Length [m]	2.0	0.602 (0.5÷1)	2.0	1.3

Table 2: Elastic mechanical properties of MARVAL 18 steel bars

Temperature 20°C	E_b [GPa]	υ	$R_{0,2}$ [MPa]	ρ_b [Kg /m^3]	$c_b = \sqrt{E_b / \rho_b}$ [m/s]	$Z_b = \rho_b c_b = \sqrt{\rho_b E_b}$ [Kg/m^{2}s]
MARVAL 18	186	0,33	1840	8000	4821,82	$38,57 \cdot 10^6$

$\overline{\varepsilon}_{max} = \ln\left[1-(2v_{imp}t_{b_{ap}i}/l_0 c_b)\right]^{-1}$. Considering a cylindrical specimen with a length $l_0 = 10\ mm$ and an initial impact velocity v_{imp} = 10 *m/s* a value of $\overline{\varepsilon}_{max}$ around of 25%-50% can be obtained for $l_{bimp} \in [0.5m, 1m] \Rightarrow l_{bi} \geq 1m \div 2m$ and $l_{bi} \geq 0.5m \div 1m$. More great plastic deformations of specimen, especially for smallest impact velocities, can be obtain for shorter specimens or specimens with special or unconventional local shape as dumbbell sample or hat one. To minimize effect of the radial dispersion elastic waves and to have bars elastic deformations conditions close to the infinite wave propagation theory [7], the bars diameters d_b must to be very small as compared to the twist of striker bar lengths i.e. $d_b / c_b t_i = d_b / 2l_{bimp} \ll 1$. The Table 1 and Table 2 synthetize the chosen material and geometric characteristics of INSA Rennes Hopkinson bars in order to perform compression impact tests with large plastic deformations of material specimen at high strain rates (more than 500s^{-1} – 1000s^{-1} corresponding to $v_{imp} \in [10m/s, 30m/s]$.

2.2 Pneumatic control circuit and experimental data acquisition

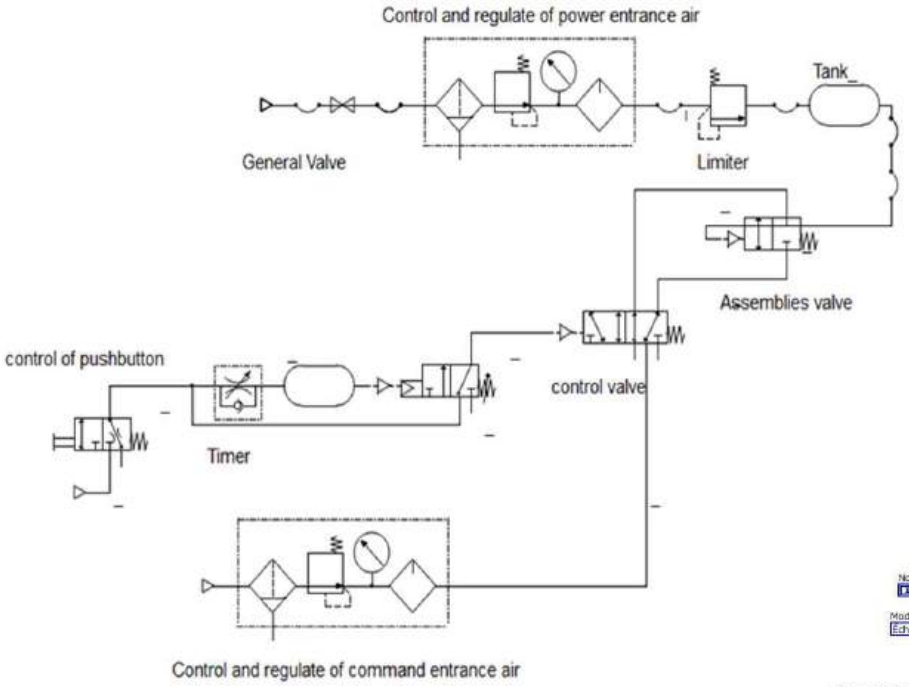

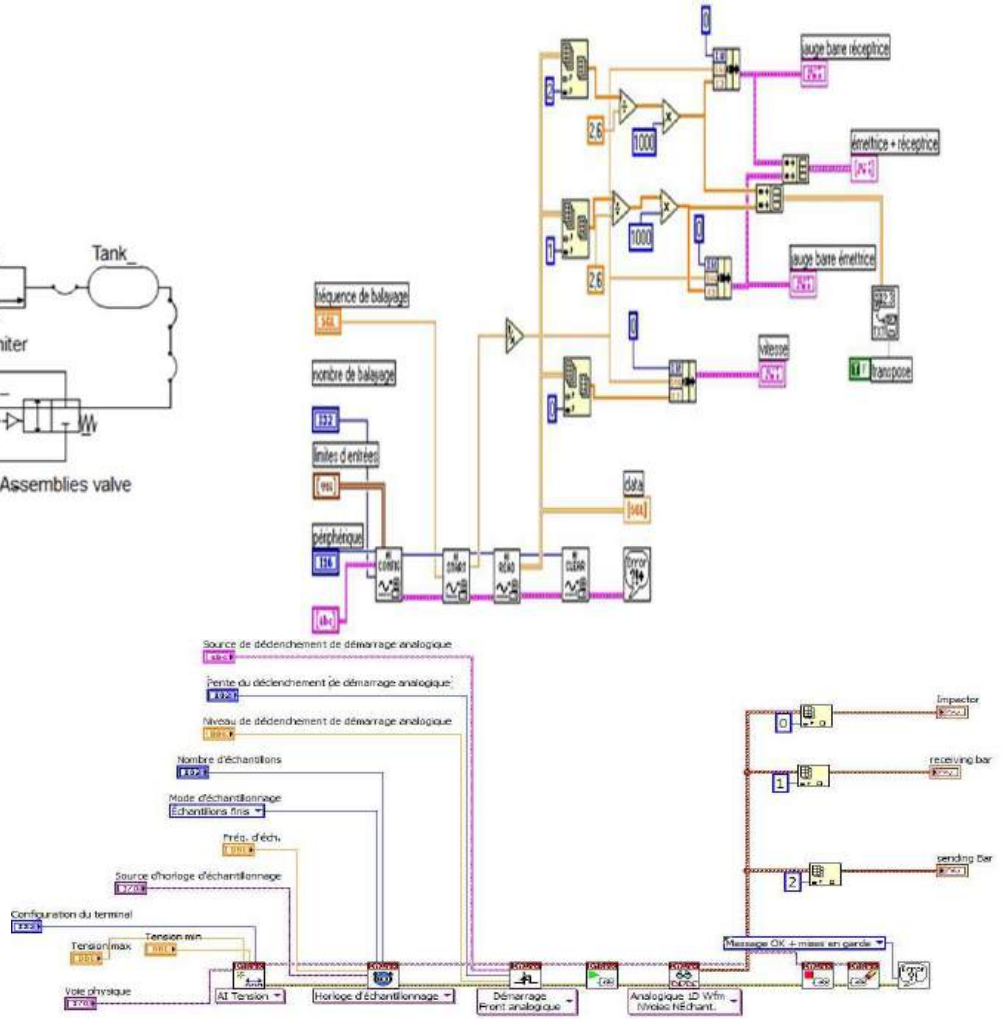

2.2 Pneumatic control circuit and experimental data acquisition

Fig.4. a) Square-Shaped Dirac tension signal of laser optical camera recorded by triggering option using Labview program, b) Gauges tension signal variation corresponding to the elastic wave deformation of the incident bar ($\varepsilon_i(t)$, $\varepsilon_r(t)$ for red curve) and sending bar ($\varepsilon_t(t)$ for blue curve) correspoding to a set tank air pressure of 1,9 bars - 2 bars [16]

$$v = \lambda_v / T_v \approx 10\,m/s \qquad \lambda_v = 5\,mm$$

$$K_{exp} = \varepsilon / \hat{U} \ (\mu def / Volt) \qquad \varepsilon \approx 2\hat{U} \cdot 10^6 / U_0 G F_g (1+\upsilon)$$

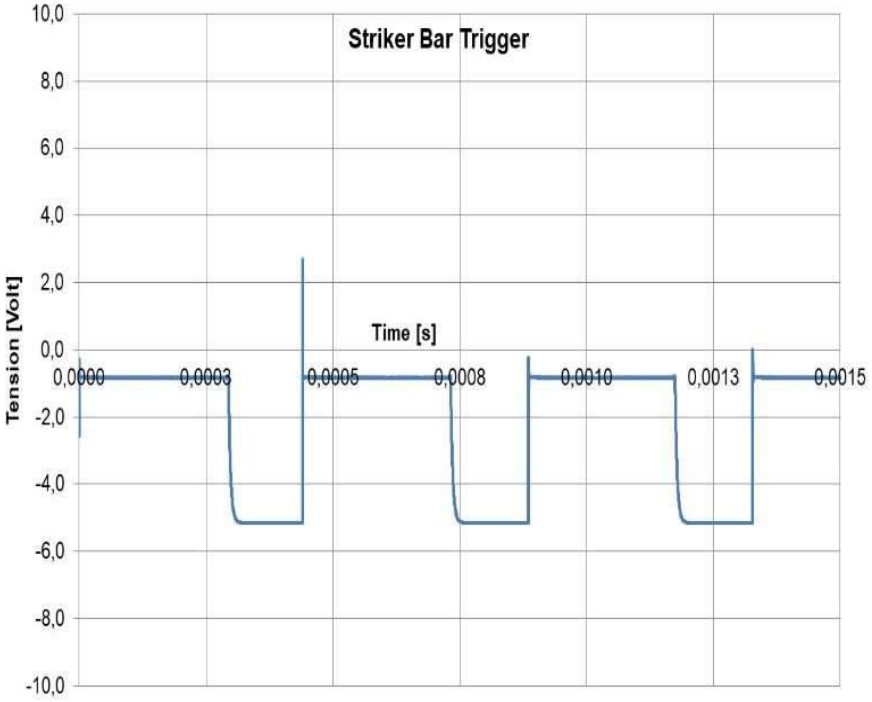

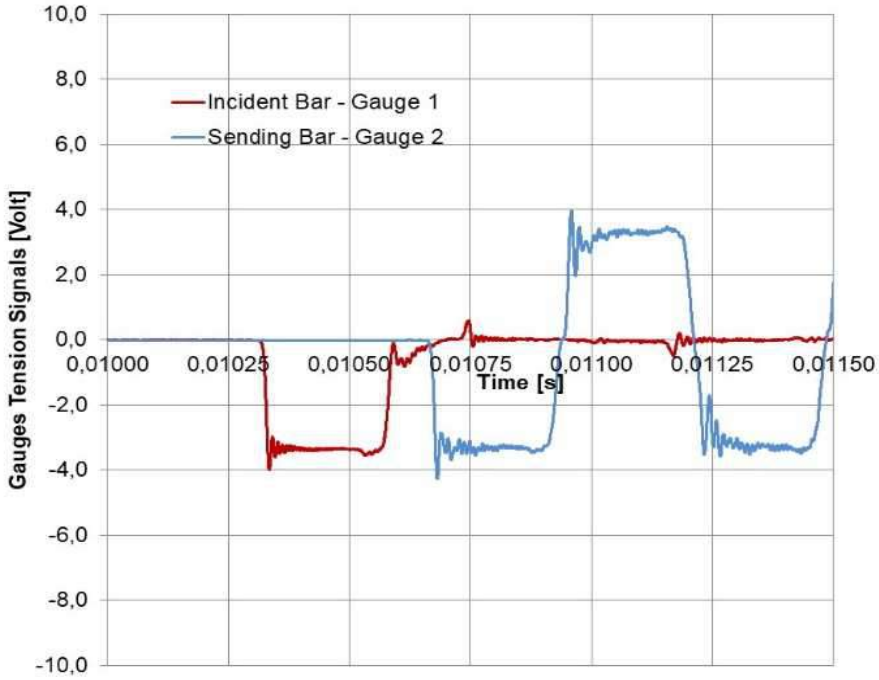

2.3 Experimental estimation of initial impact velocity using Hermite interpolation method

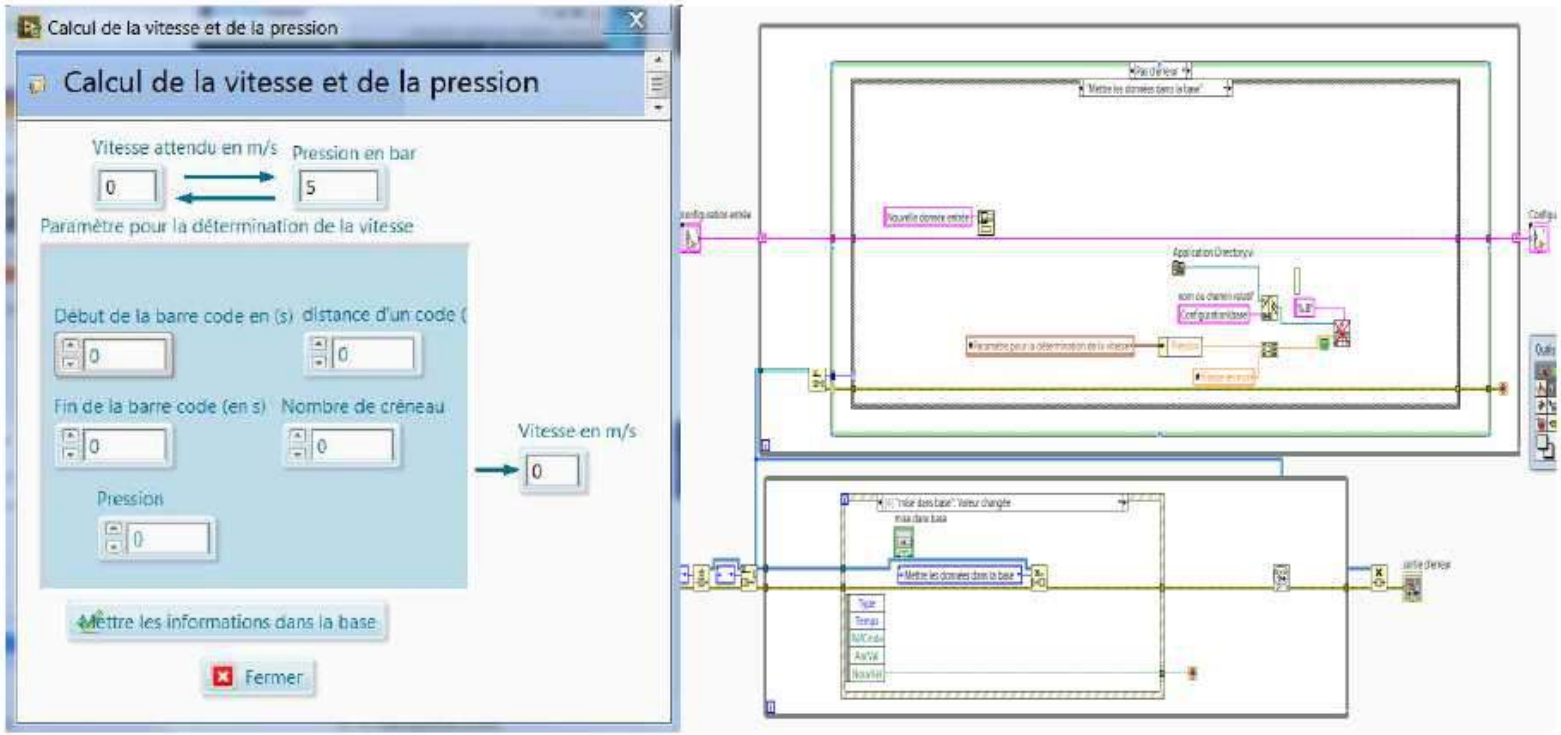

2.3 Experimental estimation of initial impact velocity using Hermite interpolation method

$$P_i(x) = f(x_i) + (x - x_i)\left[f'(x_i) - q'_i(x_i) f(x_i) \right]$$

$$q_i(x) = \prod_{j=0, j\neq i}^{j=n} \left(\frac{x - x_j}{x_i - x_j} \right)^2$$

$$P(x) = \sum_{i=0}^{n} q_i(x) P_i(x)$$

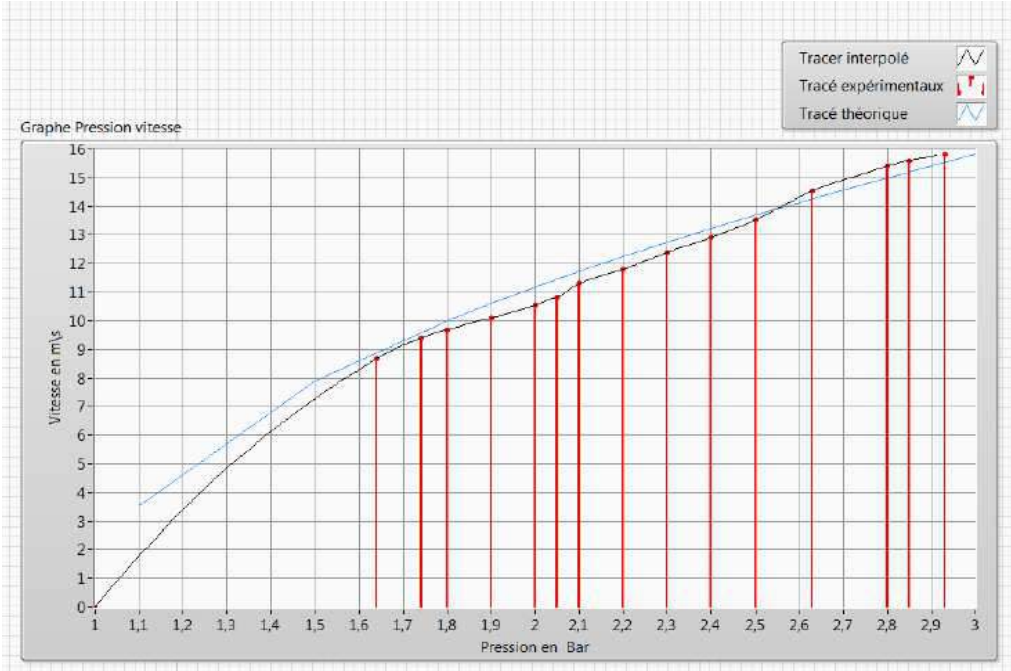

2.4 Theoretical estimation of initial impact velocity "*v*"

$$\Delta E_c + E_f = \frac{1}{2} m v^2 + E_f = W = \int_0^l \left(\iint p(x) dS \right) dx$$

$$p(x)\left(V_0 + Sx\right) = p_r V_0$$

$$W = \int_0^l p(x) S dx = \int_0^l \left(\frac{p_r V_0 S}{V_0 + Sx} \right) dx = p_r V_0 \ln\left(1 + \frac{lS}{V_0}\right)$$

$$\Delta E_f = \int_0^L F_f dx',\ F_f = \mu \pi D n_f,\ n_f = p(x) \exp\left(-4\mu x' / D\right),\ E_f = \int_0^l \Delta E_f dx$$

$$v = \sqrt{\frac{2V_0}{m} \ln\left(1 + \frac{lS}{V_0}\right) \exp\left(-4\mu L / D\right)} \cdot \sqrt{(p_c - p_0)}$$

$$v = \left(\alpha' / \sqrt{l_{imp}}\right) \sqrt{(p_c - p_0)}$$

2.4 Theoretical estimation of initial impact velocity "*v*"

l_{imp} = 0,602 m

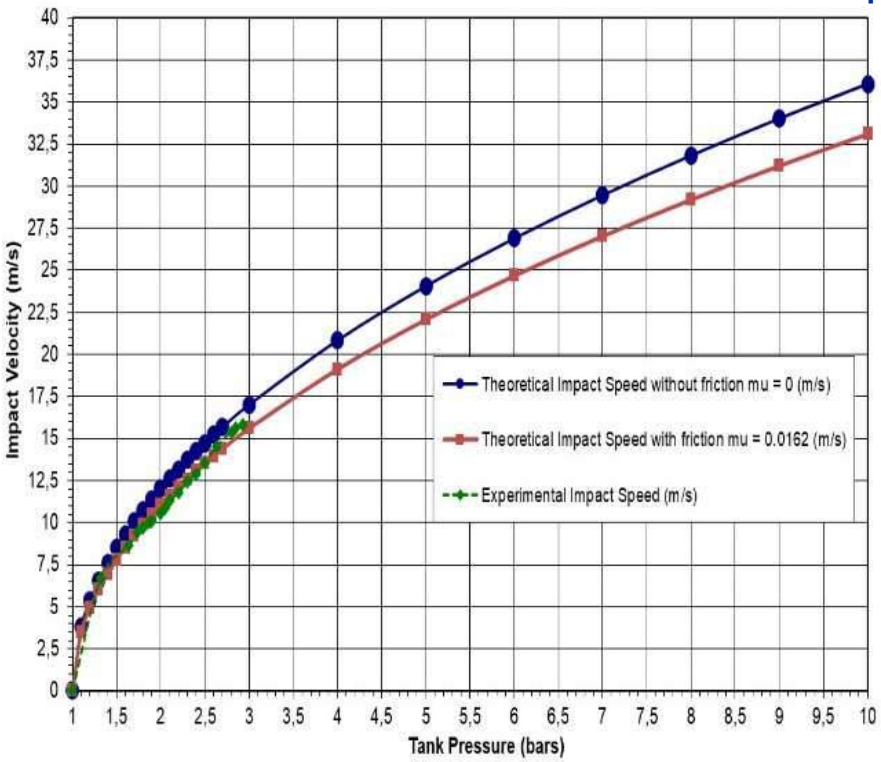

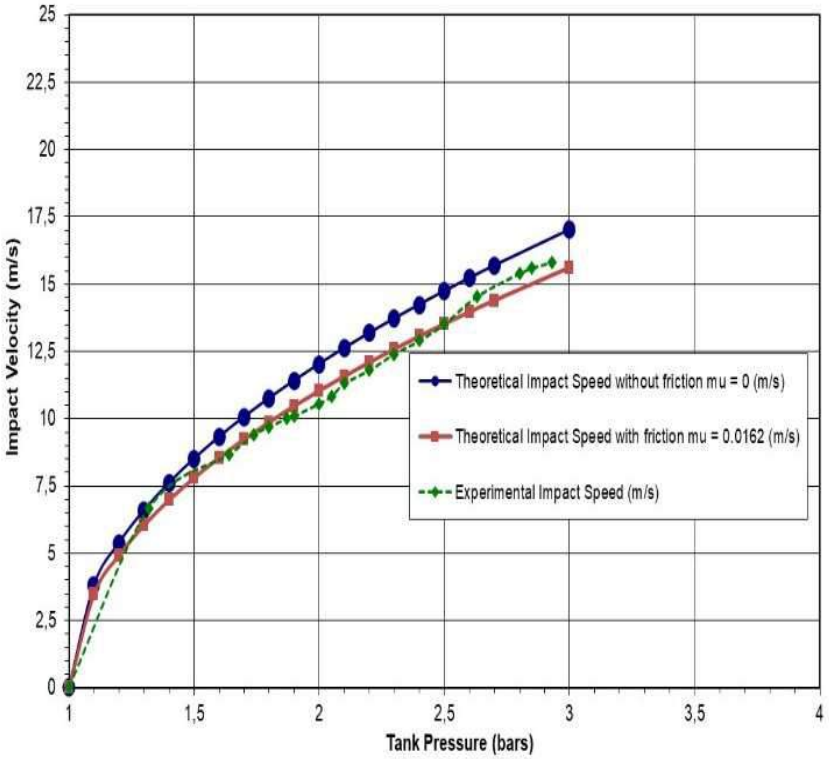

$$\underset{\mu}{Min}\left[\left(\sum_{i=1}^{N\exp}\left(v - v^{\exp}\right)^2\right) / \sum_{i=1}^{N\exp} v^{\exp\,2}\right]$$

μ = 0,0162

The identification error of friction coefficient is around of 3%.

2.4 Theoretical estimation of initial impact velocity "*v*"

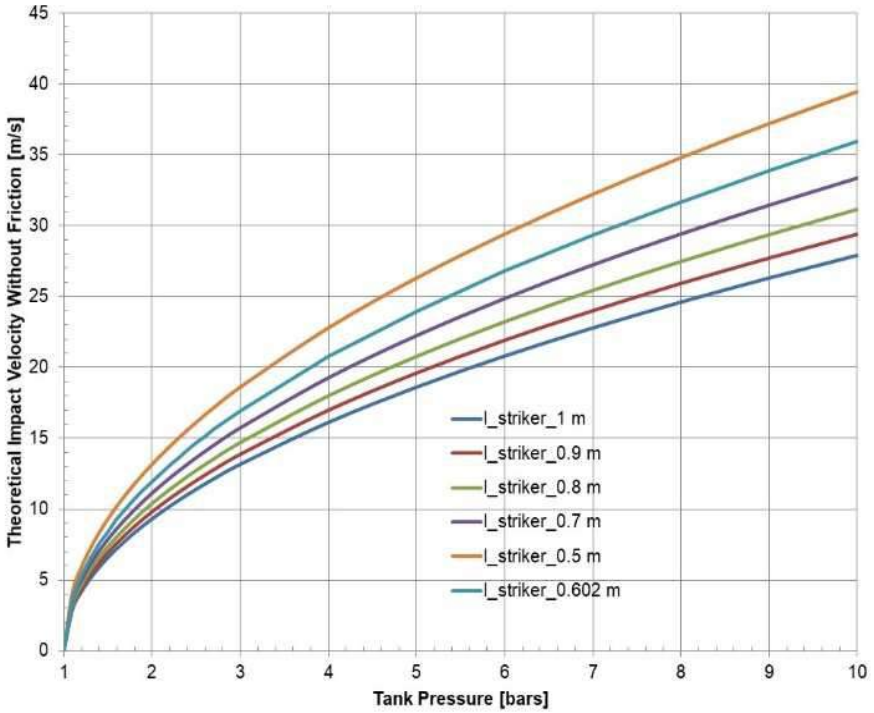

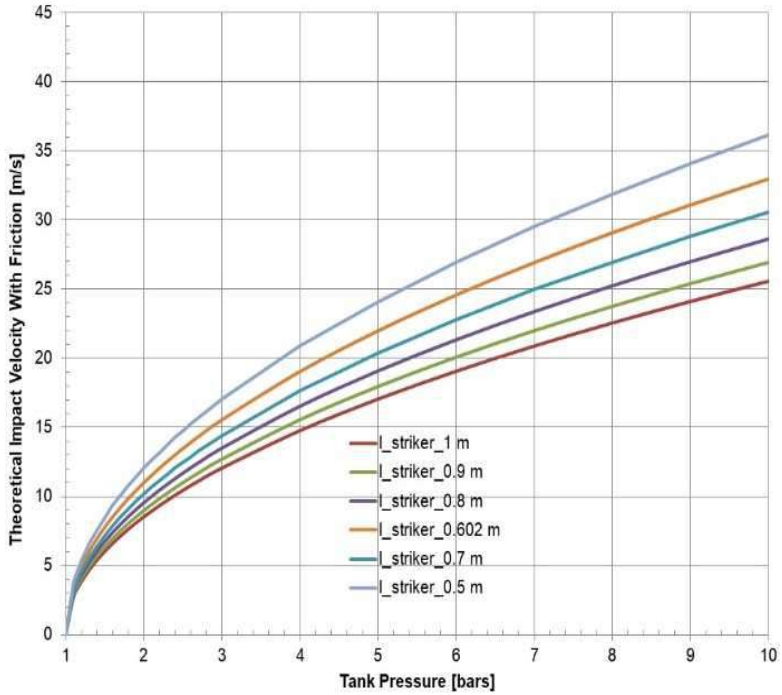

$\mu = 0$

$\mu = 0{,}0162$

An average estimation error of 8 % is obtained o

3. Numerical Analysis

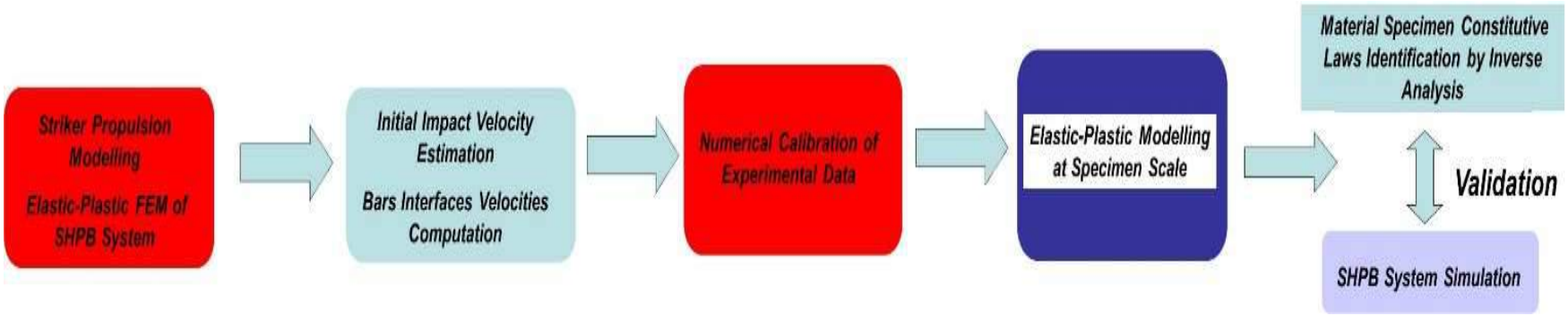

An axisymmetric dynamic Finite Element Modelling of SHPB test choosing an initial impact velocity of 10 *m/s* and an incremental time of 10^{-6}s is performed using Cast3M [18], ABAQUS and LS-Dyna code [9-13, 14-15] based on tridimensional elastic properties of the bars, inertial effect and QUAD4 mesh (Figure 10).

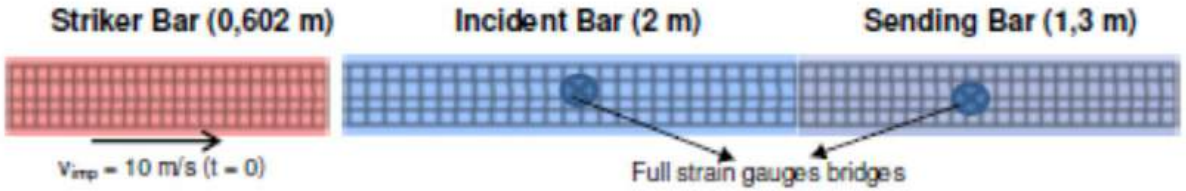

Fig.10. Mesh of the striker, incident and sending bars used for a Dynamic Finite Element Simulation of the SHPB device using Cast3M, Abaqus and LS-Dyna code

3.1 Numerical Calibration and FEM of SHPB System

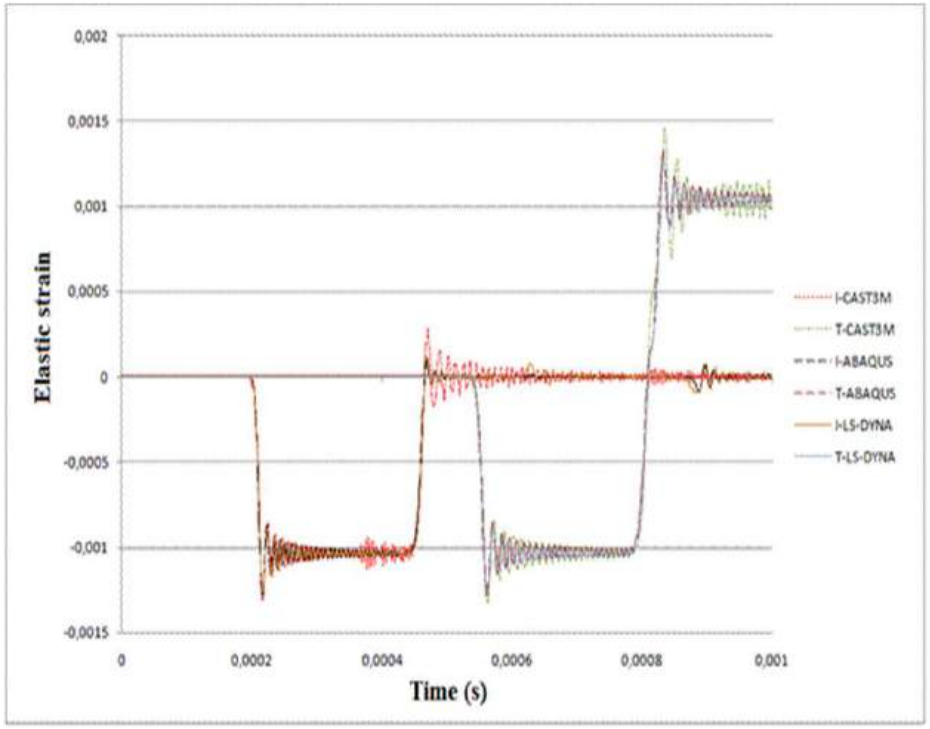

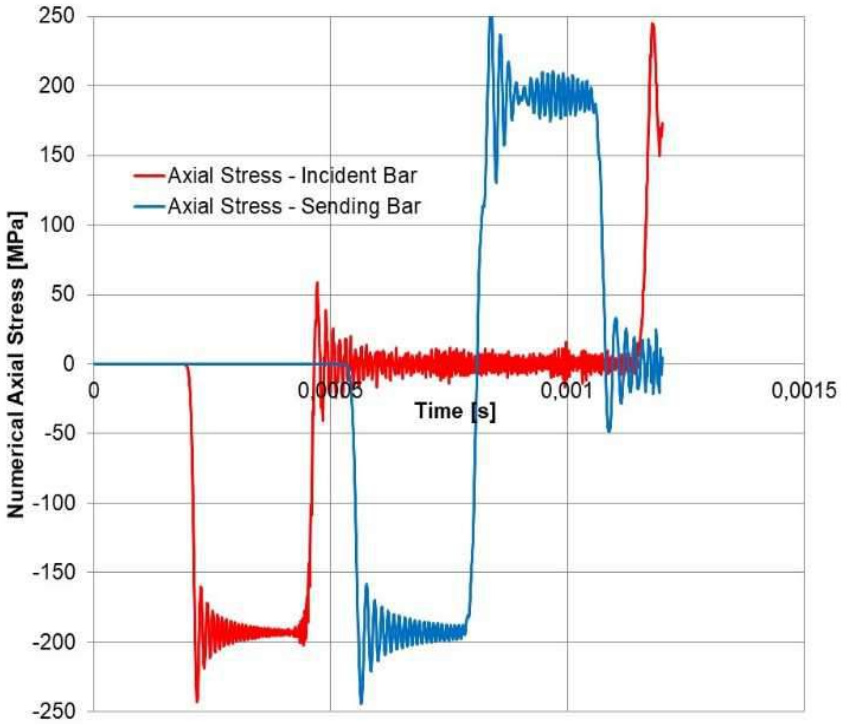

$$K_{an} = v \cdot 10^6 / 2c_{exp}\hat{U}_i \ (\mu def / Volt)$$

$$K_{num} = \hat{\varepsilon}_{i\_num} / \hat{U}_i \ (\mu def / Volt)$$

K_{exp} = 384,62 μdef /Volt. K_{an} = 317 μdef /Volt K_{num} = 310,7 μdef /Volt

3.2 Numerical Inverse Analysis of SHPB System

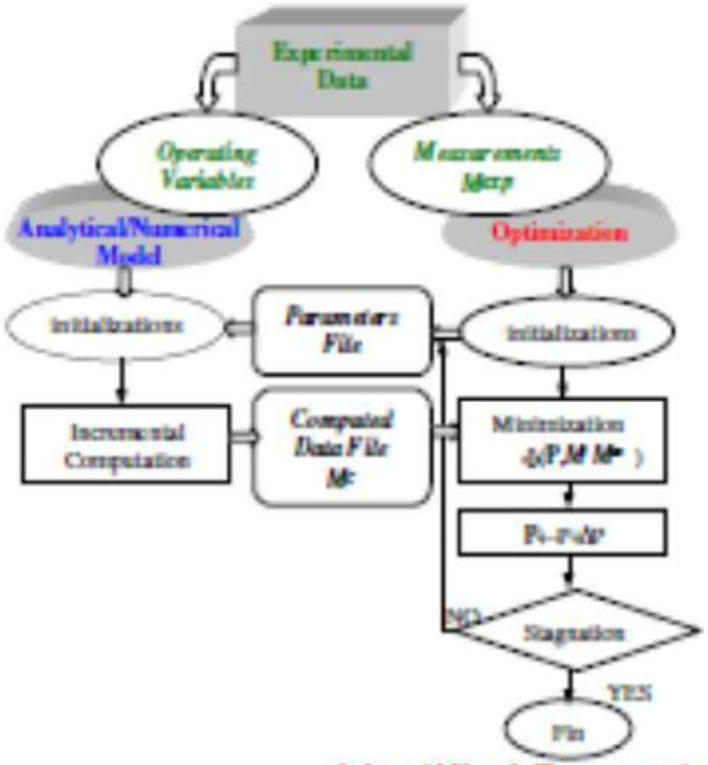

Identified Parameters P

$$\Phi(P)=\frac{\sum_{k=1}^{Ncap}\left[M^{c}(P)-M^{ex}\right]^{2}}{\sum_{k=1}^{Ncap}\left[M^{exp}\right]^{2}}$$

or

$$\Phi(P)=\sum_{k=1}^{Ncap}\left[\frac{\left(M^{c}(P)-M^{ex}\right)}{M^{ex}}\right]^{2}$$

GAUSS-NEWTON OR LEVENBERG-MARQUARD MINIMISATION ALGORITHM

$$[\Delta P]=-\left[\frac{d^{2}\Phi}{dP^{2}}\right]^{-1}\left[\frac{d\Phi}{dP}\right]$$

SHPB TEST

(Gavrus, 2000-2008 – HDR; Caestecker, 2003; Davoodi, 2006 – PhD Thesis LGCGM)
(collaboration with Mechanical Laboratory of Tampere University - Finlande)

CLASSICAL PRINCIPLE OF COLD OR HOT SHPB UPSETTING

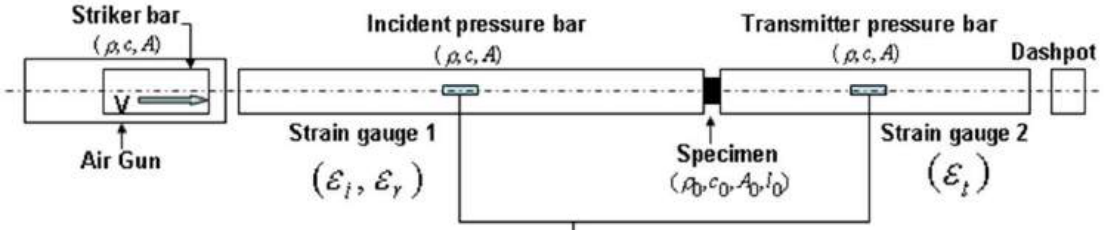

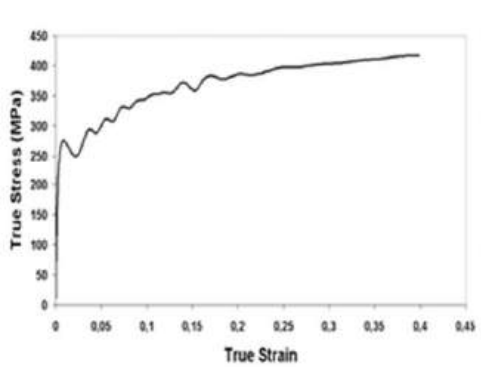

(c)

Digital oscilloscope

PC (Labview)

Specimen Stress, Strain & Strain rate

(a)

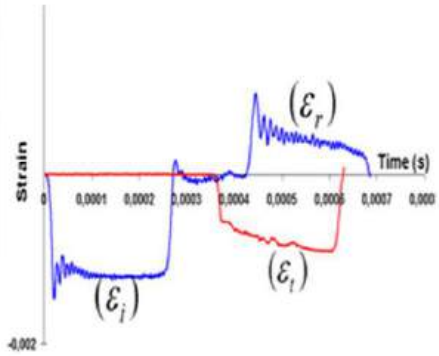

(b)

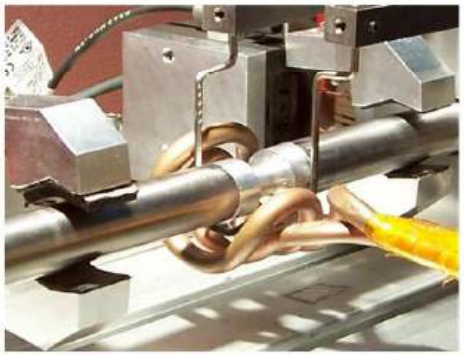

Classical Analytical Analysis using Elastic Wave Theory to estimate

$$\overline{\sigma}^{exp}, \overline{\varepsilon}^{exp}, \dot{\overline{\varepsilon}}^{exp}$$

- *Neglecting the contact friction and the heterogeneity of the deformation*
- *Use of non-linear REGRESSION to identify law parameters*

FEM SIMULATION AND INVERSE ANALYSIS OF SHPB TEST

COMPLETE NUMERICAL SIMULATION

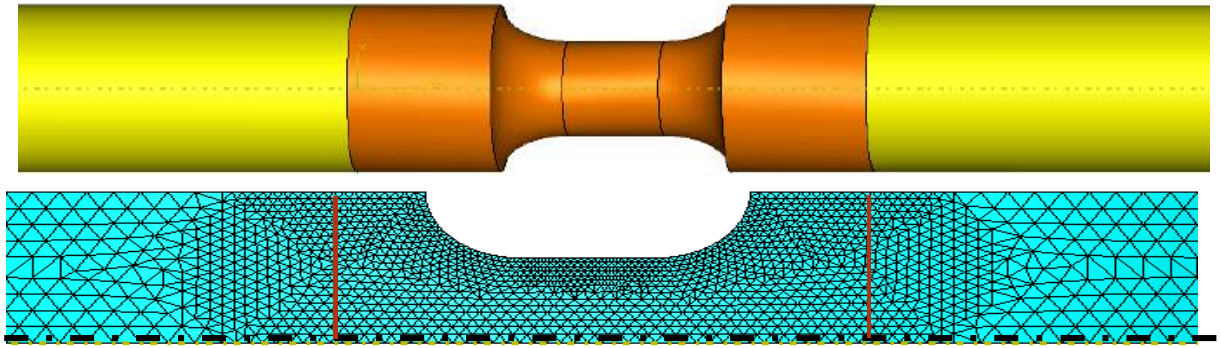

THERMAL SIMULATION (*CAST3M*)

(Initial Heating: 500°C and Cooling 10 s)

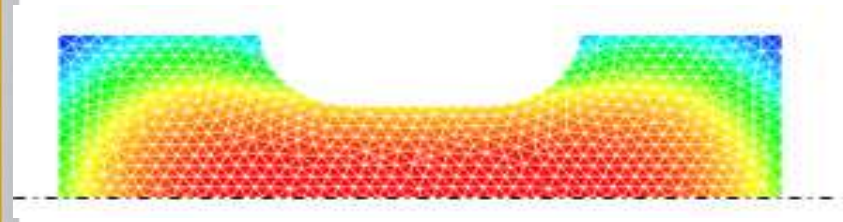

(Tmax = 483.72 °C, Tmin = 482.723°C)

INVERSE ANALYSIS OF A REDUCED MODEL (*FORGE2®*)

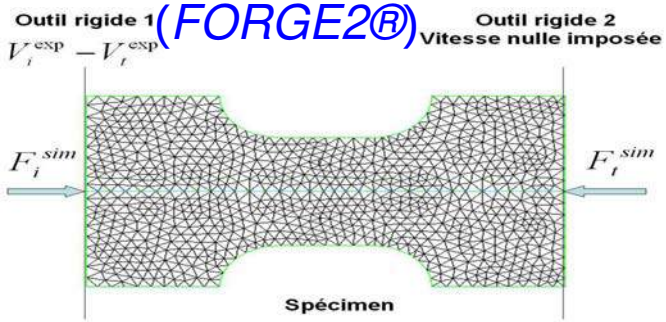

$$Q(P) = \frac{\sum_{K=1}^{M}\left[F_{i_K}^{sim}(P) - F_{i_K}^{ex}\right]^2}{\sum_{K=1}^{M}\left[F_{i_K}^{ex}\right]^2} + \frac{\sum_{K=1}^{M}\left[F_{t_K}^{sim}(P) - F_{t_K}^{ex}\right]^2}{\sum_{K=1}^{M}\left[F_{t_K}^{ex}\right]^2}$$

PARAMETER IDENTIFICATION BY INVERSE ANALYSIS OF THE SHPB REDUCED MODEL

Parameters Identified Values using different constitutive laws (Johnson-Cook, Cowper-Symonds, ASH, …) for the AA5083 aluminium alloy (*A= σ_{00} = 142 MPa, T_r=293 °K, T_m=933 °K)*

		Parameters P								Q (%)	Nb Iter
		B	**n_0**	**n_1**	**n**	**C_0**	**C_1**	**C**	**m**		
Law I (JC)	Init.	500,	-	-	0,250	-	-	0,001	2,00	29	
	final	**118,**	**-**	**-**	**0,281**	**-**	**-**	**0,093**	**1,935**	**7,07**	10
Law II	Init.	118,	0,280	0,00	-	0,090	0,00	-	1,930	7,17	
	final	**122,**	**0,504**	**-0,0005**	**-**	**0,166**	**-0,0002**	**-**	**2,996**	**6,99**	7
Law III	Init.	500,	-	-	1,00	-	-	0,001	2,00	13,9	
	final	**98,6**	**-**	**-**	**14,382**	**-**	**-**	**0,073**	**1,969**	**6,61**	17
Law IV	Init.	98,6	14,380	0,00	-	0,073	0,00	-	1,970	6,62	
	final	**99,3**	**1,936**	**0,026**	**-**	**0,148**	**-0,0002**	**-**	**4,692**	**6,29**	16
Law V	Init.	120,	-	-	0,300	-	-	0,100	2,000	15,9	
	final	**82,4**	**-**	**-**	**0,401**	**-**	**-**	**0,104**	**1,970**	**7,47**	11
Law VI	Init.	82,4	0,400	0,00	-	0,100	0,00	-	1,970	7,53	
	final	**108**	**1,083**	**-0,0015**	**-**	**0,224**	**-0,0003**	**-**	**1,975**	**7,12**	10

COMPLETE SIMULATION USING AN IMPLICITE NUMERICAL FEM (FORGE2®)

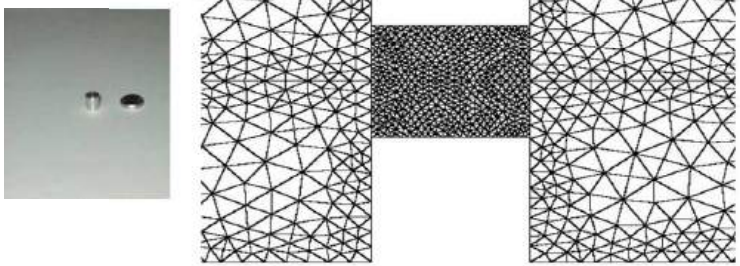

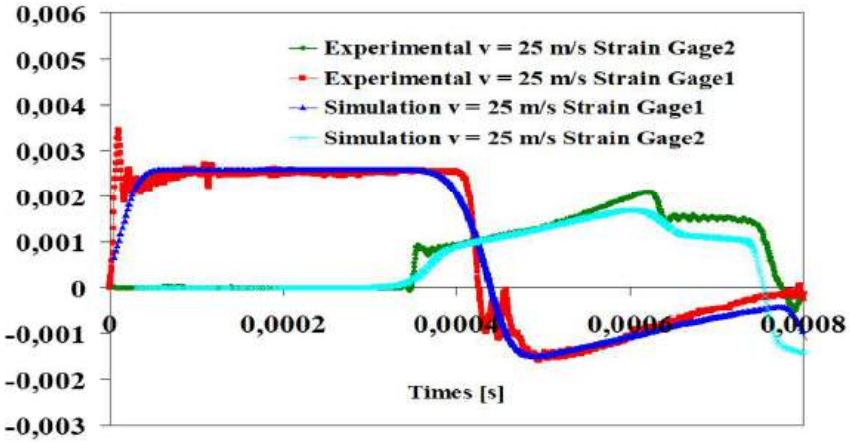

COMPARAISON BETWEEN COMPLETE MODEL (a) AND REDUCED MODEL (b)

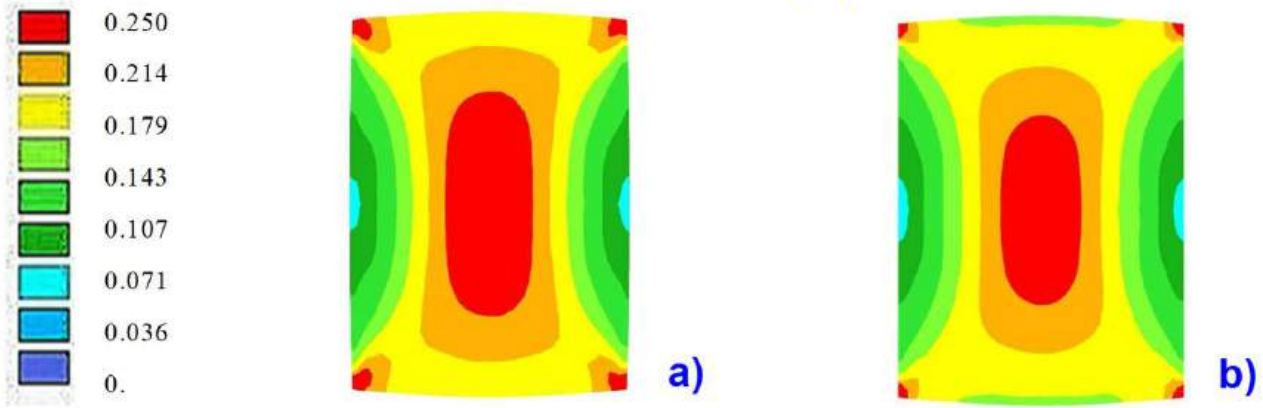

COMPLETE SIMULATION USING AN EXPLICITE NUMERICAL FEM (ABAQUS)

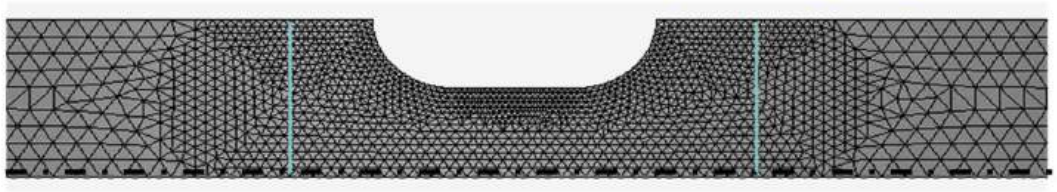

$$\bar{\sigma} = [142 + 118{,}68\bar{\varepsilon}^{0{,}2814}][1 + 0{,}093 Ln\dot{\bar{\varepsilon}}][1 - (\frac{T - 293}{933 - 293})^{1{,}935}]$$

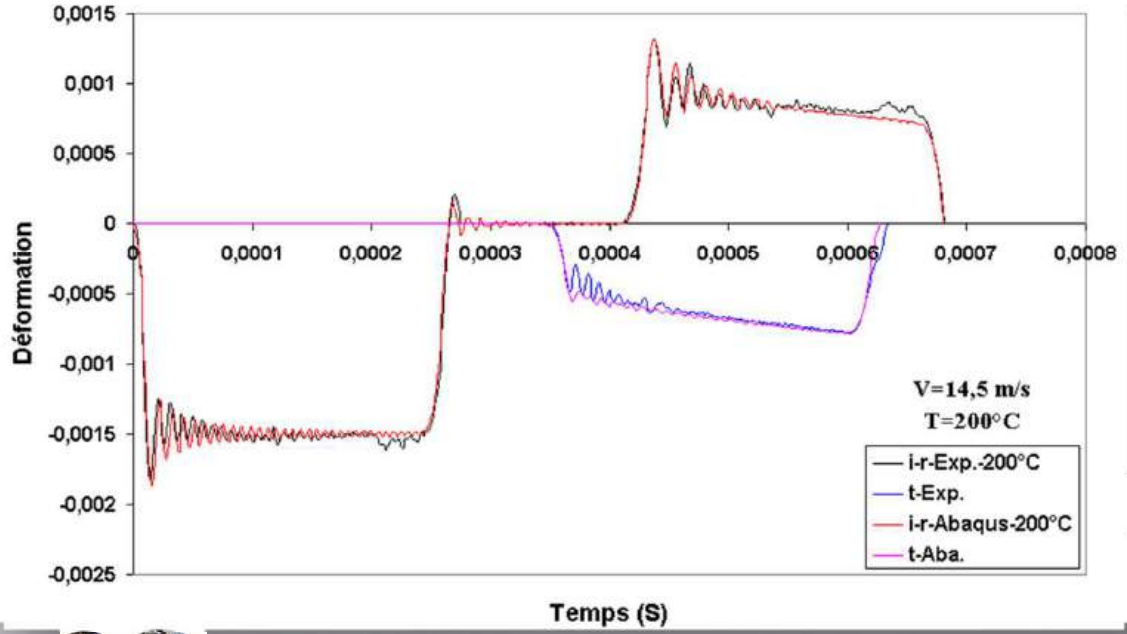

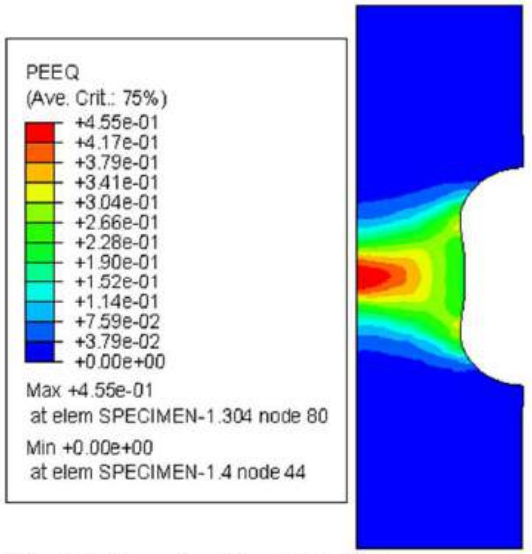

V=14,5 m/s, T=200 °C

SHPB Finite Element Simulations

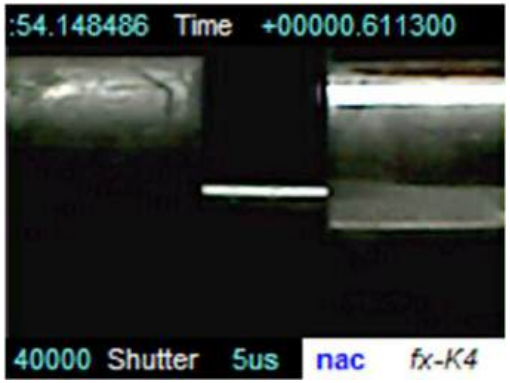

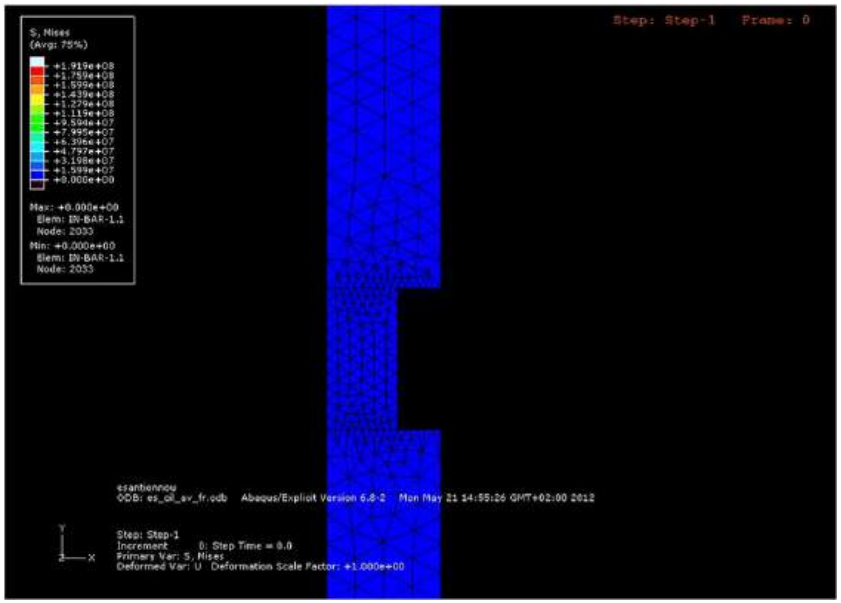

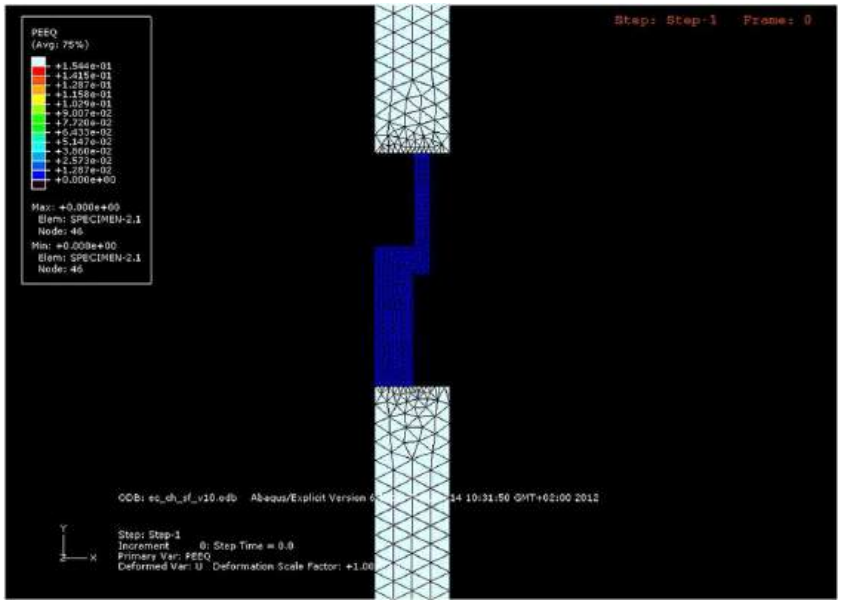

Applications to High Speed Machining

$$\sigma = \left(\sigma_0 + B \times \left[1 - \exp(-n \times \varepsilon)\right]^{n_0}\right) \times \left(1 + ASH\left[0.5 \times \left(\frac{\dot{\varepsilon}}{\dot{\varepsilon}_0}\right)^C\right]\right)$$

$$\times \left(\left[1 - k \times \left(\frac{T - T_R}{T_M - T_R}\right)^m\right]^j\right) \quad if\ T_R \le T < T_R + (T_M - T_R)\left(\frac{1}{k}\right)^{\frac{1}{m}}$$

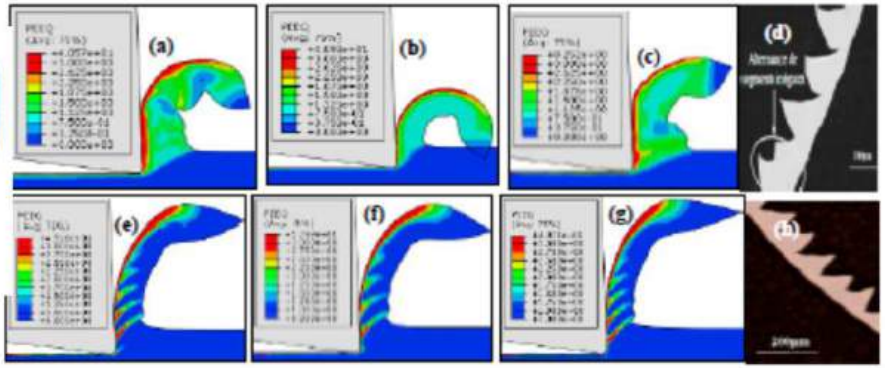

60 m/min

180 m/min

60 m/min

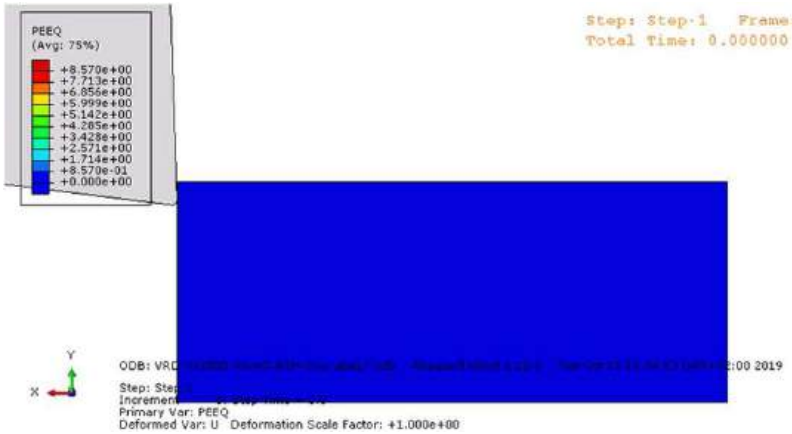

180 m/min

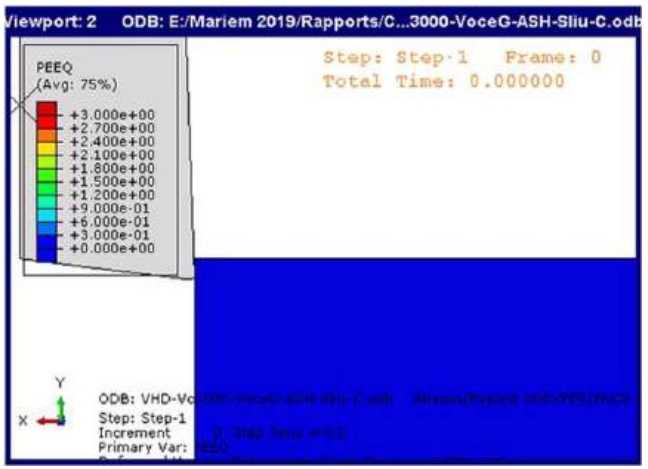

1. Conclusion and Perspectives

- The above experimental design and quantitative description of the pneumatic compression mechatronic SHPB bench confirms the robustness of impact speeds control together with strong validations of their theoretical dependency on tank air pressure set.
- A new hybrid analytical-numerical calibration method was detailed in order to can estimate the elastic wave strains which travels with a specific celerity the incident and sending bars.
- A complete dynamic Finite Element Modelling and Simulation of the SHPB system without specimen has been performed to establish a more rigorous estimation of the conversion factor between the measured gauge full bridge tension and real elastic strain value.
- Comparisons with analytical formula based on elastic wave propagation theory of infinite bars have shown the high precision of the Finite Element Modelling results, which permit to valid the entire calibration strategy.
- It is also possible to confirm again the rightness of the proposed Two-Step Inverse Analysis technique developed from 1998 during previous research works at INSA Rennes to identify specific constitutive equations of metallic materials under severe loadings and complex deformation paths: large plastic strains, high strain rates, temperature influence and important local gradients of thermo-mechanical variables.
- Regarding the generality of the proposed numerical calibration method, this one will be apply in a future research work to improve the SHPB acquisition system by use of local Bragg optic fibers sensors and specific optical interrogators developed by Dimione Systems of France and Redondo Optics Company of USA to measure in a more accuracy manner the elastic deformations of the bars.

REFERENCES

References

[1] B. Hopkinson, "A method of measuring the pressure produced in the detonation of high explosives or by the impact of bullets", Philosophical Trans. of the Royal Society of London, Vol. A213, pp. 437-452, 1914;

[2] R.M. Davies, "A critical study of Hopkinson pressure bar", Philosophical Transactions of the Royal Society of London, Vol. A240, N° 821, pp. 375-457,1948;

[3] H. Kolsky, "An investigation of the mechanical properties of materials at a very high rate of loading", Proceedings of the Physical Society of London, Vol. B62, pp.676-701, 1949;

[4] H. Kolsky, "Stress Waves in Solids", Clarendon Press, Oxford, 1953.

[5] D. J. Parry, P. R. Dixon, S. Hodson, N. A. Maliky, "Stress equilibrium effects within Hopkinson bar specimens', Department of Physics, Loughborough, 1994.

[6] G. Gary, H. Zhao, "Dépouillement de l'essai aux barres de Hopkinson par une technique de calcul inverse", Journal de Physique I (supplément J. of Physique III), Colloque C8, Vol. 4, septembre 1994;

[7] H. Zhao, "Analyse de l'essai aux barres d'Hopkinson:Aplication a la mesure du comportement dynamique des materiaux", PhD Thesis, Ecole Polytehnique, Paris, France, 1992;

[8] DAVID software, Ecole Polytehnique, LMS, Paris, France;

[9] A. Gavrus, J –P. Le Baron, P. Caestecker, E. Ragneau. "Investigation of High Speed Behaviour of Ductile Materials by Computer Simulation and Hopkinson Experimental Test", Int. Conf. on Advances in Mechanical Behaviour, Plasticity and Damage, EUROMAT 2000,Tours, France, 7-9 Nov., 2000.

[10] A. Gavrus, P. Caestecker, E. Ragneau, B; Davoodi, "Analysys of the dynamic SHPB test using the finite element simulation", Journal de Physique IV, 110, 2003;

[11] B. Davoodi, A Gavrus, E. Ragneau, "An experimental and numerical analysis of heat transfer problem in SHPB at elevated temperatures", Meas.Sci.Technol, 16, pp. 2101-2108, 2005;

[12] A. Gavrus, B. Davoodi, E. Ragneau, "A study of material constitutive behaviour at elevated temperature from compressive SHPB test using an inverse analysis method", Journal de Physique IV, EDP Sciences (Eur. Phys. J), 134, pp.661-666, 2006;

[13] A. Rotariu, "Contributii privind determinarea experimentală a proprietătilor mecanice ale unor materiale în regim dynamic", PhD Thesis, Academia Tehnica Militara, Bucuresti 2007;

[14] S. Diot, D. Guines, A. Gavrus, E. Ragneau , "Two step procedure for identification of metal behaviour from dynamic compression tests", Int. Journal of Impact Engineering, Vol. 34, pp. 1163-1184, 2007;

[15] A. Gavrus, F. Bucur, A. Rotariu, S. Cananau; "Mechanical Behavior Analysis of Metallic Materials using a Finite Element Modeling of the SHPB Test, a Numerical Calibration of the Bar's Elastic Strains and an Inverse Analysis Method", International Journal of Material Forming, vol. 8, Issue 4, pp.567-579, 2015;

[16] Adinel Gavrus, Fabien Marco, Sylvain Guegan. "Experimental Design, Modelling and Numerical Calibration of a High Speed SHPB Mechatronic System Using a Pneumatic Propulsion Device", Proc. of 23th Int. Conf. on Hydraulics and Pneumatics - HERVEX 2017, Govora, Romania, 8-10 Nov. 2017.

[17] Adinel Gavrus, Sylvain , Fabien Marco. "Contrôle des Vitesses d'Impact d'un Système Mécatronique de Barres Hopkinson avec Commande Robuste de la Pression, Calibration Numérique de la Mesure des Ondes de Déformation et Analyse Inverse", CFM 2019, 26 – 30 Août 2019, Brest, France.

[18] CAST3M – Finite Element Code developed by Center of Atomic Energy CEA – France;

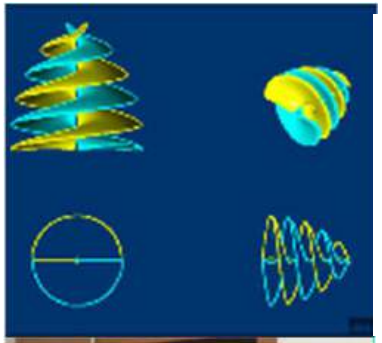

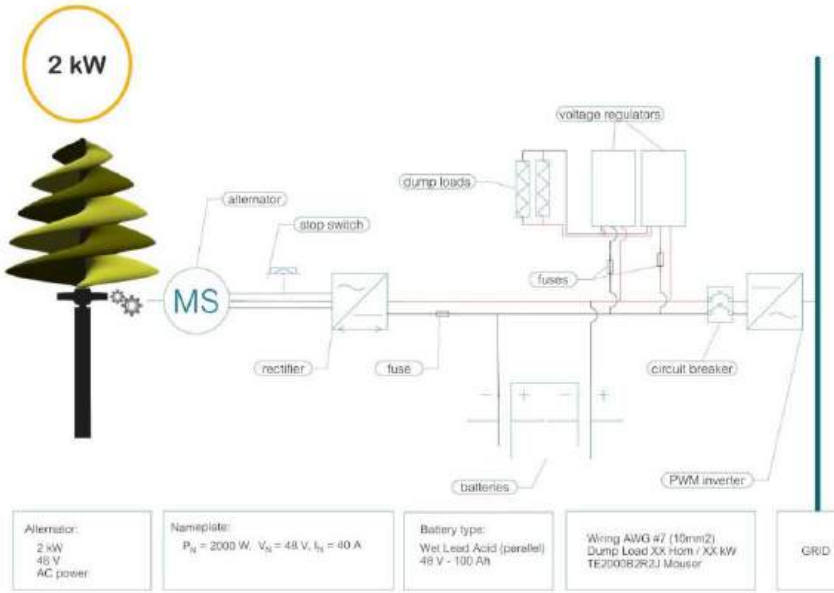
2 kW
voltage regulators
dump loads
alternator
stop switch
MS
fuses
rectifier
fuse
circuit breaker
batteries
PWM inverter
Alternator:
2 kW
48 V
AC power
Nameplate:
P_N = 2000 W, V_N = 48 V, I_N = 40 A
Battery type:
Wet Lead Acid (parallel)
48 V - 100 Ah
Wiring AWG #7 (10mm2)
Dump Load XX Hom / XX kW
TE2D00B2R2J Mouser
GRID